LAWRENCE
LIVERMORE
NATIONAL
LABORATORY

UCRL-JRNL-219802

Lanczos and Recursion Techniques for Multiscale Kinetic Monte Carlo Simulations

R. E. Rudd, D. R. Mason, A. P. Sutton

March 15, 2006

Progress in Materials Science

Disclaimer

Lanczos and Recursion Techniques for Multiscale Kinetic Monte Carlo Simulations

Robert E. Rudd [a]

[a] *Condensed Matter Physics Division, L-045, Lawrence Livermore National Laboratory, Livermore, California 94550 USA*

D. R. Mason [b] and A. P. Sutton [b]

[b] *Department of Physics, Imperial College, Exhibition Road, London, SW7 2AZ United Kingdom*

Abstract

We review an approach to the simulation of the class of microstructural and morphological evolution involving both relatively short-ranged chemical and interfacial interactions and long-ranged elastic interactions. The calculation of the anharmonic elastic energy is facilitated with Lanczos recursion. The elastic energy changes affect the rate of vacancy hopping, and hence the rate of microstructural evolution due to vacancy mediated diffusion. The elastically informed hopping rates are used to construct the event catalog for kinetic Monte Carlo simulation. The simulation is accelerated using a second order residence time algorithm. The effect of elasticity on the microstructural development has been assessed. This article is related to a talk given in honor of David Pettifor at the DGP60 Workshop in Oxford.

Key words: Lanczos, recursion, multiscale modelling, kinetic Monte Carlo, microstructural evolution
PACS:

1 Introduction

This article is part of a tribute to the extraordinary contributions David Pettifor has made to the science of materials. It involves multiscale modeling, a

Email addresses: robert.rudd@llnl.gov (Robert E. Rudd), d.mason@imperial.ac.uk (D. R. Mason), a.sutton@imperial.ac.uk (A. P. Sutton).

field in whose inception David played such an important role. It also makes use of the Lanczos recursion technique, which has been part of the mathematical underpinnings of the Bond Order Potentials which David has developed. In fact, the use of recursion in the work reviewed here is entirely due to our familiarity with it through the Bond Order Potentials. And, of course, the work was initiated while all three of the authors were part of the Materials Modelling Laboratory at Oxford University which David Pettifor founded. Thus, we hope that the presentation of this work in the Festschrift volume will honor David, particularly through these three important contributions.

Other articles in the volume explain how Lanczos recursion provides a means of calculating Green functions in tight-binding models of electronic structure [1,2], and thereby represents a key step toward quantum-based interatomic potentials, Bond Order Potentials, in which the electrons are integrated out [3,4] The principal Green function of interest is the intersite Green function

$$G_{00}(E) = \langle \Psi \left| \frac{1}{E - H} \right| \Psi \rangle \tag{1}$$

where E is the energy, H is the Hamiltonian, and Ψ is the electronic state corresponding to the bonding or antibonding orbitals (or more recently a complex linear combination of the tight-binding orbitals [4]). In the harmonic theory of elasticity, the elastic relaxation energy may be expressed in terms of an analogous lattice Green function

$$\Delta E = -\frac{1}{2} \langle f \left| \frac{1}{D} \right| f \rangle \tag{2}$$

where f_{ia} is the force on site i in direction a and D_{iajb} is the matrix of second-order potential energy coefficients. The angle brackets in this case are ordinary (finite dimensional) inner products. D is singular and the precise meaning of this expression will be discussed below. The Lanczos recursion technique again provides a powerful means of calculating the relevant energy [5] and can be used in kinetic Monte Carlo simulations of microstructural evolution including elasticity [6]. In what follows we review this methodology in some detail.

The processing of materials often relies on both the energetics that drives the system toward equilibrium and kinetic constraints that limit the rate at which equilibrium is achieved. The competition between the time scale of these kinetics and the time scale of processing can lead to the formation of structures on various length scales that determine the properties of the material system. For example, the design of metal alloys often involves the choice of a trajectory through the phase diagram, achieving a particular temperature and pressure for a specific equilibrium state and then rapidly cooling the system to constrain the kinetics and produce a desirable microstructure [7]. The result can be microstructures that display organization at many different length scales. Another example is the development of epitaxial quantum dot struc-

tures through kinetic ripening processes driven by the interplay of chemical, bulk elastic and surface energies [8].

Although these processes are very different, in both cases the local processes at the smallest scales evolve toward a local equilibrium on relatively short time scales, whereas larger structures may take much longer times to equilibrate. The energies driving this evolution may be local, such as the relative free energy of a particular material phase and interfacial free energies. On the other hand, energies associated with the elastic fields of defects and microstructures are often much longer ranged. Relevant long-range forces make microstructural evolution an intrinsically multiscale problem. The additional computational cost of modeling the long ranged elastic fields atomistically can far exceed the cost of calculating the local energetics.

Here we present an overview of an approach to the simulation of the class of microstructural and morphological evolution involving both relatively short-ranged chemical and interfacial interactions and long-ranged elastic interactions.[5,6] Both types of interactions are included at each instant of time, constituting a concurrent multiscale model of the evolution [9]. The approach is based on an efficient calculation of the elastic energy using a Lanczos recursion technique and implemented in a kinetic Monte Carlo model. As a specific demonstration of how this technique works we consider an example of material processing and microstructural synthesis in which elasticity makes an important contribution to the energies driving the kinetics of microstructural evolution. The case we consider is the aging of aluminum alloys in which clusters of the minority constituents precipitate and ripen, forming nanoscale platelets. After an hour of ripening the clusters may take the form of plates 10 nm in diameter and a single monolayer thick. These plates are known as Guinier-Preston (GP-I) zones. In subsequent stages of aging the plates continue to evolve forming different nanoscale inclusions, GP-II zones and θ' phase. The inclusions obstruct dislocation flow and the resulting hardening effect is important in industry.

Age hardening was discovered by Wilm in 1906, and attributed to precipitation by Merica, Waltenberg and Scott in 1919 [10]. Remarkably the size and crystallographic orientation of these nanoscale inclusions was inferred already in 1937 independently by Guinier and Preston through diffuse x-ray scattering [11,12]. The formation of high aspect ratio inclusions was attributed to the effect of elasticity soon thereafter. Nabarro studied the case of inclusions with incoherent interfaces and observed that second phase particles could minimize their elastic energy by forming a high-aspect-ratio plate [13]. In the intervening years there has been extensive experimental and modeling work on age hardening precipitates [14–16]. More recent x-ray [17,18], transmission electron microscopy (TEM) [19,20], and atom probe [21–23] studies have given a very precise understanding of the structure of inclusions in a broad variety of

aged alloys. Computer modeling approaches have included phase field (Cahn-Hilliard) models [24,25] and lattice kinetic Monte Carlo models [26]. Phase field models account for elasticity, typically by calculating the elastic energy using a Green function in Fourier space, but they have difficulty modeling atomistic processes such as vacancy diffusion affected by interaction with point substitutional defects. Kinetic Monte Carlo models are able to model atomistic processes, but accurate calculation of elastic energy in a lattice-based model is difficult, a point we consider below. Here we review an atomistic model of the formation of the copper clusters using kinetic Monte Carlo allowing off-lattice relaxation to account for elastic energy. [5,6] We place emphasis on an efficient means of calculating the elastic energies.

2 Elastic Effects in Diffusion

The system of interest involves the diffusion of a vacancy through an initially random binary alloy, such as Al-4 wt% Cu, with perhaps a ternary component such as Mg as well. The addition of a third component is known to affect the rate and form of the microstructural evolution. [18] We use kinetic Monte Carlo to calculate the evolution due to the reordering of the constituents as a result of vacancy diffusion [26], making the assumption that vacancy-mediated diffusion is dominant. We also assume that vacancies only hop to nearest neighbor sites through the exchange of a neighboring atom into the site of the vacancy, effectively moving the vacancy to the vacated site. We do not allow for collective processes in which the vacancy might effectively hop to a second nearest neighbor site, or farther still. There is no evidence for such processes being relevant in bulk diffusion in aluminum alloys. In order to compute the relative probability of the vacancy hopping to one site vs. another, it is necessary to know the change in energy, which for our purposes includes the change in elastic energy. The hopping rate Γ_{ij} from site i to site j is given by

$$\Gamma_{ij} = \Gamma_0(T)e^{-\Delta E/kT} \tag{3}$$

where Γ_0 includes the attempt frequency and an Arrhenius factor dependent on the height of the barrier for unbiased hops. The change in potential energy is ΔE. We used the Flynn formula for Γ_0 based on continuum elasticity [27,6], but we note that the form of the transition rate in a tilted potential is more general, albeit not exact.

The challenge is that elastic forces extend over a long range, so they are computationally expensive to compute. More precisely, the cost of obtaining the relaxed structure and its energy for any one vacancy hop is a few orders of magnitude greater than the cost for the corresponding unrelaxed energy. That extra cost, compounded by the number of possible hops and the many millions

of steps needed during the simulation, can be prohibitive and keep simulations from reaching the relevant time scales of late stage microstructural evolution.

One strategy for computing the requisite energies is to precompute the energy of each possible state of the system. For an A-B alloy with N sites of which N_a are type A and one is a vacancy, the total number of possible configurations is $N!/[N_a!(N - N_a - 1)!]$. We are interested in systems with about 10 000 atoms in order to minimize finite size effects on the elasticity, so precomputation of the entire configuration space is infeasible. If a subset of the system consisting of N_{sub} sites were precomputed, then the number of configurations would be $2^{N_{sub}}$. The number of atoms within the range of the potential during a hop is 27, and for $N_{sub} = 27$, there are 134 million configurations, and this precomputation does not account for the long-ranged elasticity. Instead of precomputing, we must calculate the hopping rates on the fly, including elasticity.

3 Elasticity in Microstructural Evolution

There are two aspects of the elasticity problem that require consideration. The first is the long-ranged elastic fields that are created by the hopping vacancy as well as precipitates in the Al matrix. The second aspect is the elastic relaxation of the atoms in the proximity of the vacancy. Whereas the long-ranged elastic fields obey linear, albeit mildly anisotropic, elasticity, the near-field relaxation can be quite non-linear due to the differences in the atomic sizes (the ratio of atomic volumes for Al:Cu:Mg is 1.0:0.71:1.4) as they relax around the vacancy. Both aspects of elasticity make significant contributions to the energies biasing vacancy diffusion, so both must be treated seamlessly within a successful multiscale model of the system.

In order to pose a well defined problem for the development of such a multiscale model, we have taken the energetics of a particular classical atomistic model as our gold standard. The interatomic potentials have been devised to reproduce some of the elastic and chemical properties of Al-Cu-Mg alloys, although they by no means are expected to reproduce the subtleties of the alloy phase diagram. Other forms of atomistic energetics have been used to study aging, including cluster expansions based on density functional theory [28–30].

We have used the interatomic potentials developed by Mason et al. [5]. The potentials are similar in form to Finnis-Sinclair [31] and Sutton-Chen [32] interatomic potentials, with a shorter range (4.5Å, which is between the second and third nearest neighbor shells) imposed by an exponential cutoff. The form is

$$E = \frac{1}{2}\sum_i \sum_{j\neq i} v\left(r_{ij}\right) - \sum_i \sqrt{\rho_i} \tag{4}$$

$$\rho_i = \sum_{j\neq i} \phi\left(r_{ij}\right) \tag{5}$$

$$v\left(r\right) = a_{ij}\left(\frac{r}{r_0}\right)^{-m_{ij}} \exp\left(\frac{c_{ij}}{r - r_c}\right) \tag{6}$$

$$\phi\left(r\right) = b_{ij}\left(\frac{r}{r_0}\right)^{-n_{ij}} \exp\left(\frac{c_{ij}}{r - r_c}\right) \tag{7}$$

where r_{ij} is the distance between atoms i and j and $r_c = 4.5$Å is the cutoff. a_{ij}, b_{ij}, c_{ij}, m_{ij} and n_{ij} are parameters that depend on the type of atoms i and j. The values of the coefficients are given in Ref. [5]. In practice, it is useful to store the pair potentials as functions of r^2, tabulated as spline functions (cf. Ref. [33]).

3.1 Harmonic Elastic Relaxation

We are interested in computing the change in elastic energy associated with a vacancy hop. We can compute the energy, its first derivative, the force on each atom f_{ia}, and its second derivative, the stiffness matrix D_{iajb}. D is also known as the force-constant matrix and is related to the dynamical matrix in real space. Here the indices $i, j, \ldots$ run over the N atomic lattice sites and the indices $a, b, \ldots$ run over the dimensions. The elastic energy in the quasiharmonic approximation is given by

$$E_{elastic} = E_0 + \frac{1}{2}\sum_{ijab} u_{ia} D_{iajb} u_{jb} - \sum_{ia} f_{ia} u_{ia} + \sum_{ia} \lambda_a u_{ia} \tag{8}$$

where E_0 is the energy associated with the reference state $u = 0$. The system is translationally invariant, reflected in the sum rule

$$\sum_i D_{iajb} = 0. \tag{9}$$

The three Lagrange multipliers λ_a are introduced in order to impose the constraint that the center of mass remain fixed: $(1/N)\sum_i u_{ia} = u_a^0$ in each dimension. This constraint is needed to make the formulation well defined.

At equilibrium, the elastic energy is minimized with respect to variations in u_i, and hence

$$f_{ia} = D_{iajb} u_{jb} + \lambda_a. \tag{10}$$

Summing over i using the equation for translational invariance (9), we find

$$\lambda_a = (1/N)\sum_i f_{ia} \tag{11}$$

and we can solve the equilibrium equation as

$$u_{ia} = \left(D'_{iajb}\right)^{-1} (f_{jb} - \lambda_b) + u^0_a \tag{12}$$

where D'_{iajb} is the sub-block of the stiffness matrix excluding the three translational zero modes, $f_{ia} = \text{const}$. The full stiffness matrix is singular because of these zero eigenvalues, but the submatrix is non-singular and the inverse in Eq. (12) is well defined. Finally, we have the elastic energy (8) at equilibrium

$$E_{elastic}|_{equilibrium} = E_0 - \frac{1}{2} \sum_{ijab} \tilde{f}_{ia} \left(D'_{iajb}\right)^{-1} \tilde{f}_{jb} \tag{13}$$

where $\tilde{f}_{ia} = f_{ia} - \lambda_a$. This form of the elastic energy was mentioned in the introduction (2). It involves a lattice Green function analogous to the electronic Green function used in the construction of Bond Order Potentials (1), and we make use of this analogy in implementing the Lanczos technique to calculate the energy.

4 The Lanczos Algorithm

The Lanczos algorithm is a technique to transform a matrix H_{ij} into an equivalent tri-diagonal form [34,35]. For our purposes, H_{ij} is the stiffness matrix, but we keep the discussion general for now. The algorithm works as follows. Specify a starting vector $v_i^{(0)}$ and define $v_i^{(-1)}$ to be zero. Consider the recursion relation

$$b_{n+1} v_i^{(n+1)} = \sum_j H_{ij} v_j^{(n)} - a_n v_i^{(n)} - b_n v_i^{(n-1)}. \tag{14}$$

The Lanczos vectors $v_i^{(0)}$ are to be orthonormal,

$$\sum_i v_i^{(n)*} v_i^{(m)} = \delta_{nm} \tag{15}$$

where the Kronecker delta, δ_{nm}, is one if the indices are equal and zero otherwise. Using this property, and taking the inner product of Eq. (14) with $v_i^{(n+1)}$, $v_i^{(n)}$ and $v_i^{(m)}$, respectively, leads to

$$b_n = \sum_{ij} v_i^{(n-1)*} H_{ij} v_j^{(n)} \tag{16}$$

$$a_n = \sum_{ij} v_i^{(n)*} H_{ij} v_j^{(n)} \tag{17}$$

$$0 = \sum_{ij} v_i^{(m)*} H_{ij} v_j^{(n)} \quad \text{for } |m-n| > 1 \tag{18}$$

Suppose H_{ij} is real and symmetric (like the stiffness matrix), then the Lanczos basis is real and $\sum_{ij} v_i^{(n)} H_{ij} v_j^{(n-1)} = b_n$, too. Thus in the basis $\{v^{(n)}\}$ the matrix H_{ij} has diagonal entries a_n and first sub- and super-diagonal entries b_n, and all other entries zero. This tri-diagonal representation $\tilde{H}_{ij}$ of the matrix is useful for many purposes [35,1].

For our application, the matrix H_{ij} is the stiffness matrix (where the indices i and j now run over the $3N$ dimensions of the direct product of the sites and dimensions), which is singular because it has 3 zero modes associated with translation invariance in 3D, as mentioned above. One might expect that some care would be needed in treating D or its non-singular relative D'. It is interesting to note that the Lanczos algorithm works even for a singular matrix, the distinction between D and D' is irrelevant, a property that we now show. In generality, consider an H_{ij} that is block diagonal and v_i^0 that is in the vector subspace associated with one block. Then $H^n v^0$ is also in the same block subspace, for any value of n. Each vector generated in the recursion (14) is in the block subspace. Thus, the Lanczos tridiagonal form is actually only the tridiagonal form for the block. In the case of a singular matrix, the zero eigenmode is its own block subspace and hence does not mix with the non-singular block. It is only the non-singular block that is tri-diagonalized. Similarly, as we turn to the computation of the inverse, it is only the inverse of the non-singular block that is calculated. We note that the Lanczos coefficients are related to the moments of H_{ij}:

$$\mu^{(n)} = v^{(0)*} H^n v^{(0)} \tag{19}$$

$$= \sum_{i_1, i_2, \ldots, i_{n-1}} v^{(0)*} H v^{(i_1)} v^{(i_1)*} H v^{(i_2)} \ldots v^{(i_{n-1})*} H v^{(0)} \tag{20}$$

where the identity matrix has been inserted in the form of a sum over direct products of the complete Lanczos basis vectors, and the result may be recognized as combinations of Lanczos coefficients. This fact has been used to great advantage in the Bond Order Potentials, but we do not make use of it in the elastic problem.

4.1 Diagonal Matrix Elements of Green Function

For our purposes, the most important application is the calculation of matrix elements of the inverse of the tridiagonal $\tilde{H}_{ij}$. The formula for the first element of the inverse, $\tilde{H}_{00}^{-1}$, may be easily computed using Kramer's rule, and the well known continued fraction formula is [1]

$$\sum_{ij} v_i^{(0)} H_{ij}^{-1} v_j^{(0)} = \tilde{H}_{00}^{-1} \tag{21}$$

$$= \cfrac{1}{a_0 - \cfrac{b_1^2}{a_1 - \cfrac{b_2^2}{a_2 - \cfrac{b_3^2}{a_3 - \cdots}}}} \tag{22}$$

The first vector, $v_i^{(0)}$, is taken to be the normalized force, $v_i^{(0)} = f_i/|f|$. The relaxation energy is then $-(1/2)|f|^2 \tilde{D}_{00}^{-1}$. According to the argument that the zero modes decouple, the standard stiffness matrix can be used to compute the Lanczos coefficients in $\tilde{D}_{00}^{-1}$; i.e. it is not necessary to compute D' explicitly. The expression (22) may be truncated at the desired level of accuracy, and it is not necessary to compute the entire Lanczos basis.

Were all of the a_k identical and all of the b_k identical, then the continued fraction (22) would reduce to a simple closed-form expression. For example,

$$T = \cfrac{b^2}{a - \cfrac{b^2}{a - \cfrac{b^2}{a - \cdots}}} \tag{23}$$

$$= \frac{1}{2}\left(a - \sqrt{a^2 - 4b^2}\right) \tag{24}$$

When the recursion is taken to a specified level, rather than setting all of the higher a_k and b_k values to zero, they can be set equal to the final value and the resulting continued fraction can be replaced by the closed-form expression (24). The use of this square-root terminator is known to improve the convergence. We use 6-12 levels of recursion with the square-root terminator [5].

4.2 Off-diagonal Green Function Matrix Elements in the Lanczos Basis

Other matrix elements of H_{ij}^{-1} may be of interest. For example, since $v_j^{(0)} = f_j/|f|$, the displacement is given by

$$u_i = |f|\, D_{ij}^{-1} v_j^{(0)} + u_a^0 \tag{25}$$

$$= |f|\, \tilde{D}_{k0}^{-1} v_i^{(k)} + u_a^0 \tag{26}$$

where the indices of the Green function on the second line are in the Lanczos basis, as indicated by the tilde over D. Thus, the displacement is related to the first row of the Green function matrix elements.

These off-diagonal matrix elements may also be calculated easily using Kramer's rule, but there is actually a faster technique [5]. Suppose we have computed

$\tilde{D}_{00}^{-1}$, perhaps including a terminator as described in the next section. Then the other matrix elements of the first row must satisfy the equation

$$\begin{pmatrix} a_0 & b_1 & 0 & 0 & \dots \\ b_1 & a_1 & b_2 & 0 & \dots \\ 0 & b_2 & a_2 & b_3 & \dots \\ \dots & & & & \end{pmatrix} \begin{pmatrix} \tilde{D}_{00}^{-1} \\ \tilde{D}_{01}^{-1} \\ \tilde{D}_{02}^{-1} \\ \dots \end{pmatrix} = \begin{pmatrix} 1 \\ 0 \\ 0 \\ \dots \end{pmatrix} \tag{27}$$

This equation taken row by row is equivalent to the following recursion relationships:

$$b_1 \tilde{D}_{01}^{-1} = 1 - a_0 \tilde{D}_{00}^{-1} \tag{28}$$

$$b_k \tilde{D}_{0k}^{-1} = -a_{k-1} \tilde{D}_{0k-1}^{-1} - b_{k-1} \tilde{D}_{0k-2}^{-1} \quad (k > 1) \tag{29}$$

At each step of the recursion, the right-hand side of the equation is known, so the first row may be determined by this *scalar* recursion relation. Since the Green function is a symmetric matrix, once the first row is known, it provides the matrix elements needed to generate the second row and so on. It is interesting to note that $\tilde{D}_{00}^{-1}$ (and hence the terminator) enters linearly into the ultimate expression for each matrix element.

4.3 Lanczos Recursion for Anharmonic Lattices

As indicated above, the difference in the atomic sizes of the constituents of aluminum alloys is great enough for anharmonic effects to be important. We have used a quasiharmonic approach in order to apply the Lanczos recursion technique to a system in which the harmonic approximation is not sufficient [5]. The displacement is computed according to Eqs. (26) and (29); then the stiffness matrix is recomputed at the new displacement and another iteration of 6-12 levels of Lanczos recursion is applied, and so on until convergence is attained. The result is not as elegant as in the harmonic case, but it performs comparably to the best pre-conditioned conjugate gradient techniques for relaxation [36].

5 Simulation Results

The results from simulations of the evolution of Al-Cu-Mg alloy microstructures have been reported in detail in Refs. [5] and [6]. Here we focus on those

results that are most directly linked to the question of elastic effects.

Kinetic Monte Carlo simulations [37,38] were run as follows. The event catalog consisted of vacancies hopping from one face-centered cubic lattice site to a nearest neighbor site, with the elementary rate determined by Eq. (3) including the elastic energy change computed using the anharmonic Lanczos technique. A second order residence time algorithm [39,6] was used to accelerate the kinetic Monte Carlo by integrating out non-productive 'flicker' events; i.e. events in which the vacancy hops to a neighboring site and then as its next move hops back to the starting location. Flicker events do not cause the microstructure to change, but they do contribute to the rate at which the microstructure evolves. The second-order technique [6] calculates the rate catalog exactly summing over these flicker events so that they do not need to be modeled explicitly. In simulations in which the vacancy arrives at a greatly preferred site (e.g. at a compressive dilatation source or a high energy interface), many flickers may take place before the vacancy breaks free, and the second order algorithm provides a significant acceleration of the simulation. Also the energies of recently visited configurations were stored in case those configurations were visited again (in a higher order flicker) (cf. [40]).

The simulation is run starting from a random alloy configuration consisting of about 10 000 atoms in a 3D periodic simulation box. At each step an event is selected at random from the catalog and time is advanced stochastically according to the total rate. Different measures of clustering are computed in order to analyze the development of the microstructure in the system.

5.1 Range of the Elastic Field

Elastic fields are long ranged. In continuum elasticity the displacement field around a point dilatation source decreases like $1/r^2$ away from the source [41]; the stress and strain decrease like $1/r^3$; and the energy density in a shell of fixed solid angle decreases like $1/r^4$. Vacancies are point dilatation sources, but in analyzing the volume of influence it is important to recognize that it is the change in energy during the hop that is important. The monopole moment is either conserved or very nearly conserved during the hop; it is the dipole moment that changes. As the vacancy hops (or more precisely the atom hops to fill the vacancy, creating another vacancy in its wake), a certain amount of dilatation is taken from one site and transferred to the other. This is a dipole change, and in linear elasticity the change it creates in the field is a dipole field. Its displacement field decreases like $1/r^3$ away from the source; the stress and strain decrease like $1/r^4$; and the energy density in a shell of fixed solid angle decreases like $1/r^6$. As an aside, this argument is related to the reason why it is impossible to determine where charged particles are located within

a black hole and only their total charge can be measured outside the horizon [42].

Thus, one might expect that a reasonably small cluster of atoms would be affected. In practice, we have found that a cluster of 754 atoms in which the anharmonic Lanczos technique is used to 6-12 levels of recursion is sufficient to guarantee convergence of the energy to better than 1 meV. The cluster calculation was compared against the fully relaxed energy of the full 10 000 atom system [5].

While we are using a cluster to calculate the energy of the locally relaxed structure, this technique is not equivalent to the cluster expansions employed in other studies [29,30]. Those works used first-principles calculations to parameterize a generalized Ising model with pairwise interactions out to third nearest neighbors and a few many-body interactions. The data used to parameterize the Ising model consist of first-principles calculations of the total energies of a few dozen ordered compound configurations (large supercells). To the Ising model energies are added a coherency energy. Their mixed-space cluster expansion has the significant advantage of more accurate local energetics, but it does not achieve our principal goal of including the long-range and non-linear elasticity. The use of the Lanczos technique captures the local non-linear elastic relaxation. Also, because the current displacement field is used as the starting point for the relaxation, the Lanczos technique captures elastic interactions beyond the range of the cluster.

5.2 Effect of Elasticity on Vacancy Diffusion

One driving force for vacancy diffusion across long length scales is the pressure gradient. Vacancies are sources of dilatation, and find it energetically favorable to be in regions of high compressive stress. Typically, pressure variations are not large, however. In inhomogeneous systems like the alloys of interest here, it is the change in the local configuration that biases the diffusion. It is expected over the course of a long period of microstructural evolution that low elastic energy structures will form; elasticity also plays an important role in the early evolution of the system, prior to the formation of well-defined cluster geometries.

One way to observe this effect is to examine the elapsed time after a number of vacancy hops. The accumulated time is shown in Fig. 1 as a function of the number of (productive) moves of the vacancy. Two cases are shown. In the left panel is plotted the result for a flexible lattice; i.e. the case when elasticity is included in the hopping rate. In the right panel is plotted the corresponding result without elastic relaxation. It is observed that the Mg atoms are much

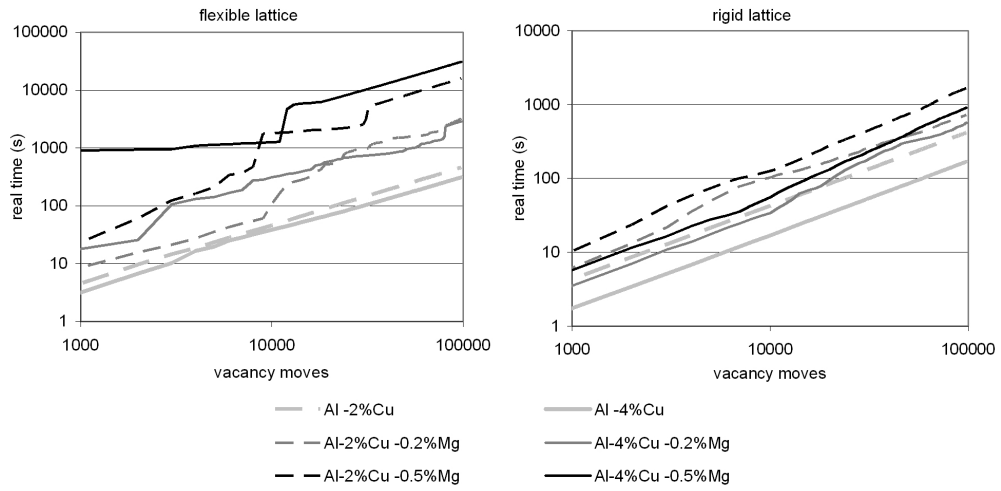

Fig. 1. Plots of the elapsed time vs. the number of vacancy moves in two cases: with elasticity (left) and without elasticity (right). After [5]. Reprinted with permission.

more effective at pinning the vacancy when elasticity is included, and hence the time evolution of the system is altered significantly even in the early stage of the evolution.

As a second measure of the effect of elasticity, we have examined the rate of cluster formation. As the system evolves, copper clusters form and ripen. The rate of formation depends on whether elasticity is included or not, as shown in Fig. 2. These results are from simulations with a single vacancy in a periodic supercell of 10 976 atomic sites, under no external stress, and at a simulated temperature of 300K. The system consisted of aluminum with 2at.%, 4at.% or 6at.% copper, as indicated in the Figure. Details about the order parameter are given in Eq. (3.1) and the surrounding text in Ref. [5]. The plots show that inclusion of elasticity increases the rate of clustering in all three alloys.

5.3 Conclusions and Outlook

We have reviewed an approach to the simulation of the class of microstructural and morphological evolution involving both relatively short-ranged chemical and interfacial interactions and long-ranged elastic interactions. The Lanczos recursion technique, part of the foundation of the Bond Order Potentials, has been used in a different context here: to determine elastic relaxation energies for kinetic Monte Carlo simulation. [5] This advance together with other algorithmic developments such as the use of a second-order residence time technique has allowed the simulation of ripening in aluminum alloys for times approaching seconds [6]. Since the elastic relaxation energy is related to a particular lattice Green function matrix element, the Lanczos technique is a

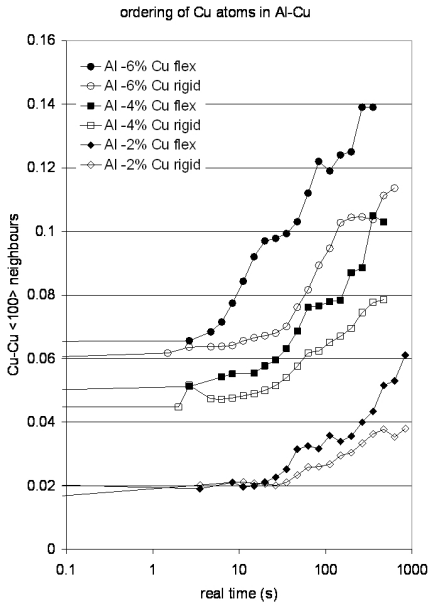

Fig. 2. Order in the aluminum-copper system. An order parameter indicating the number of neighboring copper atoms in the $\langle 100 \rangle$ directions is plotted vs. the elapsed time. Three different alloy compositions were simulated, and each with elasticity included (flex) and not included (rigid). After [5]. Reprinted with permission.

particularly natural and efficient means of calculating the energy. In simulations of vacancy-mediated diffusion and ripening in Al-Cu-Mg alloys, cluster formation was observed. Furthermore, the rate of microstructural development was moderated by the action of the Mg. The Mg atoms acted to trap the vacancy, slowing the development of the microstructure. This effect was much less pronounced in kinetic Monte Carlo simulations in which the elastic relaxation was not included, but were otherwise identical. The appreciable role of elasticity even in the very early stages of microstructural development was remarkable.

Many questions arising in this work have yet to be addressed. The techniques for calculating elastic energies and for accelerating Monte Carlo simulations are independent of the choice of potential. The optimization of the potential used in the study described here placed considerable weight on the short range of the potential and the resulting speed of calculation. It would be desirable to see these simulations repeated with a potential based on a higher fidelity description of aluminum. Also, the extension to a broader range of aluminum alloys is desirable. To date, we have not observed the formation of fully developed Guinier-Preston zones or θ' phase. Perhaps the most significant extension of this work would be to continue the simulations longer in real time, possibly through efficient parallel algorithms, and to study the self-assembly process in detail. Then the complete picture would be obtained of the influence of Mg on the vacancy-mediated diffusion and the resulting

control of the microstructural evolution during aluminum alloy aging.

Acknowledgements

This work was performed in part under the auspices of the U.S. Dept. of Energy by the Univ. of California, Lawrence Livermore National Laboratory, under Contract No. W-7405-Eng-48. DRM was supported by an EPSRC grant. The computer simulations were performed on Oswell, the Oxford University Supercomputer. DRM gratefully acknowledges the fellowship in the LLNL Summer Institute on Computational Materials Science and Chemistry through which part of this work was done. The authors would like to thank M. W. Finnis and R. Drautz for organizing the DPG60 Workshop in Oxford in July 2005.

References

[1] R. Haydock, V. Heine, M. J. Kelly, Electronic structure based on the local atomic environment for tight-binding bands, J. Phys. C 5 (1972) 2845–58.

[2] R. Haydock, The recursive solution of the Schrödinger equation, Solid State Phys. 35 (1980) 215–94.

[3] D. G. Pettifor, New many-body potential for the bond order, Phys. Rev. Lett. 63 (1989) 2480–83.

[4] D. G. Pettifor, I. I. Oleinik, Analytic bond-order potentials beyond Tersoff-Brenner. I. Theory, Phys. Rev. B 59 (1999) 8487–99.

[5] D. R. Mason, R. E. Rudd, A. P. Sutton, Atomistic modelling of diffusional phase transformations with elastic strain, J. Phys.: Condens. Matter 16 (2004) S2679–97.

[6] D. R. Mason, R. E. Rudd, A. P. Sutton, Stochastic Kinetic Monte Carlo algorithms for long-range Hamiltonians, Computer Physics Comm. 160 (2004) 140–157.

[7] R. W. Cahn (Ed.), Physical Metallurgy, North-Holland, Amsterdam, 1970.

[8] R. E. Rudd, G. A. D. Briggs, A. P. Sutton, G. Medieros-Ribiero, R. S. Williams, Equilibrium model of bimodal distributions of epitaxial island growth, Phys. Rev. Lett. 90 (2003) 146101.

[9] R. E. Rudd, J. Q. Broughton, Concurrent coupling of length scales in solid state systems, Phys. Stat. Sol. (b) 217 (2000) 251–91.

[10] R. F. Mehl, The historical development of physical metallurgy, in: Cahn [7], Ch. 1, pp. 1–31.

[11] A. Guinier, Structure of age-hardened Al-Cu alloys, Nature (London) 142 (1938) 569–70.

[12] G. D. Preston, The diffraction of x-rays by age-hardening aluminium copper alloys, Proc. Roy. Soc. A 167 (1938) 526–38.

[13] F. R. N. Nabarro, The strains produced by precipitation in alloys, Proc. Roy. Soc. London A 175 (1940) 519–38.

[14] J. B. Cohen, The internal structure of Guinier-Preston zones in alloys, Solid State Phys. 39 (1986) 131–206.

[15] S. C. Wang, M. J. Starink, Precipitates and intermetallic phases in precipitation hardening Al-Cu-Mg(Li) based alloys, Int. Mater. Reviews 50 (2005) 193–215.

[16] V. Gerold, On the structure of GP zones in Al-Cu alloys, Scr. Met. 22 (1988) 927–32.

[17] J. M. Silcock, T. J. Heal, H. K. Hardy, Structural aging characteristics of binary aluminium-copper alloys, J. Inst. Met. 82 (1954) 239–48.

[18] H. K. Hardy, The ageing characteristics of some ternary Al-Cu-Mg alloys with Cu:Mg weight ratios of 7:1 and 2.2:1, J. Inst. Met. 84 (1954) 17–34.

[19] H. Yoshida, D. J. H. Cockayne, M. J. Whelan, Study of Guinier-Preston zones in aluminum-copper alloys using weak-beam technique of electron-microscopy, Philos. Mag. 34 (1976) 89–100.

[20] J. Konno, M. Kawasaki, K. Hiraga, Direct imaging of Guinier-Preston zones by high-angle annular detector dark-field scanning transmission electron microscopy, J. El. Microscopy 50 (2001) 105–11.

[21] K. Hono, Nanoscale microstructral analysis of metallic materials by atom probe field ion microscopy, Prog. Mater. Sci. 47 (2002) 621–729.

[22] S. P. Ringer, K. Hono, T. Sakurai, The effect of trace additions of sn on precipitation in Al-Cu alloys: an atom probe field ion microscopy study, Metall. Mater. Trans. A 26 (1995) 2207–17.

[23] N. Gao, L. Davin, S. Wang, A. Cerezo, M. J. Starink, Precipitation in stretched Al-Cu-Mg alloys with reduced alloying content studied by DSC, TEM and atom probe, Mater. Sci. Forum 396–402 (2002) 923–8.

[24] A. G. Khachaturyan, Theory of Structural Transformations in Solids, Wiley, New York, 1983.

[25] A. G. Khachaturyan, S. Semenovskaya, T. Tsakalakos, Elastic strain energy of inhomogeneous solids, Phys. Rev. B 52 (1995) 15909–19.

[26] T. T. Rautiainen, A. P. Sutton, Influence of the atomic diffusion mechanism on morphologies, kinetics, and the mechanisms of coarsening during phase separation, Phys. Rev. B 59 (1999) 13681–92.

[27] C. P. Flynn, Point Defects and Diffusion, Clarendon Press, Oxford, 1972.

[28] C. Wolverton, First-principles theory of 250000-atom coherent alloy microstructure, Modell. Simul. Mater. Sci. Eng. 8 (2000) 323–33.

[29] J. Wang, C. Wolverton, S. Müller, Z.-K. Liu, L.-Q. Chen, First-principles growth kinetics and morphological evolution of Cu nanoscale particles in Al, Acta Mater. 53 (2005) 2759–64.

[30] C. Ravi, C. Wolverton, First-principles study of crystal structure and stability of Al-Mg-Si-(Cu) precipitates, Acta Mater. 52 (2004) 4213–27.

[31] M. W. Finnis, J. E. Sinclair, A simple empirical n-body potential for transition metals, Phil. Mag. A 50 (1984) 45–55.

[32] A. P. Sutton, J. Chen, Long-range Finnis-Sinclair potentials, Phil. Mag. Lett. 63 (1991) 217–24.

[33] M. P. Allen, D. J. Tildesley, Computer Simulation of Liquids, Clarendon Press, Oxford, 1987.

[34] C. Lanczos, An iteration method for the solution of the eigenvalue problem of linear differential and integral operators, J. Res. Natl. Bur. Stand. 45 (1950) 255–282.

[35] Y. Saad, Iterative Methods for Sparse Linear Systems, PWS, Boston, 1996.

[36] W. H. Press, S. A. Teukolsky, W. T. Vetterling, B. P. Flannery, Numerical Recipes in Fortran, 2nd Edition, Cambridge Univ. Press, Cambridge, 1992.

[37] A. B. Bortz, M. H. Kalos, J. L. Lebowitz, A new algorithm for Monte Carlo simulation of ising spin systems, J. Comput. Phys. 17 (1975) 10–8.

[38] K. A. Fichthorn, W. H. Weinberg, Theoretical foundations of dynamical Monte Carlo simulations, J. Chem. Phys. 95 (1991) 1090–6.

[39] M. Athènes, P. Bellon, G. Martin, Identification of novel diffusion cycles in B ordered phases by Monte Carlo simulation, Phil. Mag. A 76 (1997) 565–85.

[40] D. R. Mason, T. S. Hudson, A. P. Sutton, Fast recall of state history in kinetic Monte Carlo simulations utilizing the Zobrist key, Computer Physics Comm. 165 (2005) 37–48.

[41] J. D. Eshelby, The elastic field outside an ellipsoidal inclusion, Proc. Roy. Soc. A 252 (1959) 561–9.

[42] C. W. Misner, K. S. Thorne, J. A. Wheeler, Gravitation, W. H. Freeman, San Francisco, 1973, §32.7.